γ-ray spectroscopy of a four-quasiparticle isomer band in ^{174}Re

R. J. Carroll,[1] P. M. Walker,[1] G. J. Lane,[2] M. W. Reed,[2] A. Akber,[2] H. M. Albers,[3] J. J. Carroll,[4] D. M. Cullen,[5] A. C. Dai,[6] C. Fahlander,[7] M. S. M. Gerathy,[2] S. S. Hota,[2] G. Lotay,[1] T. Kibédi,[2] V. Margerin,[8] A. J. Mitchell,[2] N. Palalani,[2] T. Palazzo,[2] Z. Patel,[1] R. Shearman,[1,9] A. E. Stuchbery,[2] and F. R. Xu[6]

[1]*Department of Physics, University of Surrey, Guildford GU2 7XH, United Kingdom*
[2]*Department of Nuclear Physics, R.S.P.E, Australian National University, Canberra ACT 2601, Australia*
[3]*GSI Helmholtzzentrum für Schwerionenforschung GmbH, Planckstrasse 1, 64291 Darmstadt, Germany*
[4]*CCDC/Army Research Laboratory, 2800 Powder Mill Road, Adelphi, Maryland 20783, USA*
[5]*School of Physics and Astronomy, Schuster Building, University of Manchester, Manchester M13 9PL, United Kingdom*
[6]*State Key Laboratory of Nuclear Physics and Technology, School of Physics, Peking University, Beijing 100871, China*
[7]*Department of Physics, Lund University, 22100 Lund, Sweden*
[8]*School of Physics and Astronomy, University of Edinburgh, Edinburgh EH9 3FD, United Kingdom*
[9]*National Physical Laboratory, Teddington, Middlesex TW11 0LW, United Kingdom*

(Received 10 November 2019; revised manuscript received 10 March 2020; accepted 22 April 2020; published 26 May 2020)

Excited states in ^{174}Re have been populated in fusion-evaporation reactions at the Australian National University, and γ-ray spectroscopy has been used to determine the level structure and to deduce the underlying nucleon configurations. The half-life of the bandhead of the $K^\pi = 8^-$ band has been measured to be 2.7(4) ns. A band built on an isomeric state of spin-parity (14^-) and a half-life of 53(5) ns has been observed here for the first time, and has been determined to have a four-quasiparticle structure. Contrasting reduced-hindrance values for its decay are discussed in terms of deformation and configuration changes, as indicated by configuration-constrained potential energy surface calculations.

DOI: 10.1103/PhysRevC.101.054314

I. INTRODUCTION

Deformed, axially symmetric nuclei are well known to exhibit high-K isomers, where K is the angular-momentum projection on the symmetry axis [1,2]. The K value comes from one or more unpaired nucleons (quasiparticles), and γ-ray decay transitions from such states are called "K forbidden" when the change in K, ΔK, is greater than the angular momentum, λ, carried by the transition, i.e., $\Delta K > \lambda$, leading to hindered transitions and extended half-lives that range from nanoseconds to years.

The region of the nuclear chart where the majority of high-K isomers are to be found [1] centers on the well-deformed nuclide $^{178}_{72}$Hf$_{106}$, which has a four-quasiparticle, $K^\pi = 16^+$, isomer with a half-life of 31 years and an excitation energy of 2.4 MeV. However, due mainly to rotational (Coriolis) K mixing and the onset of axially asymmetric shapes, the extent of high-K isomers in the N-Z plane is limited, especially for isomers involving four or more quasiparticles. Nevertheless, their observation provides information about K-mixing mechanisms and hence the degree to which axial symmetry is preserved in high-spin states.

The present work is concerned with an odd-odd, neutron-deficient isotope of rhenium, $^{174}_{75}$Re$_{99}$. Until recently, the lightest odd-odd rhenium isotope observed with a multiquasiparticle isomer was ^{180}Re [1,3], but Guo *et al.* [4] have reported evidence for the existence of a strongly populated, four-quasiparticle isomer in ^{174}Re, with a half-life exceeding 1 μs. In this work, a new study of ^{174}Re is presented. Although a different interpretation is given, which does not involve such a long-lived isomer, a shorter-lived, weakly populated four-quasiparticle isomer is found. Furthermore, it is argued on the basis of decay hindrance factors that the isomer decay pathway is significantly influenced by shape and configuration-change effects.

II. EXPERIMENTAL DETAILS

The experiment was performed at the Australian National University (ANU) Heavy Ion Accelerator Facility [5] in which excited states in ^{174}Re were populated via the fusion evaporation reaction ^{160}Dy(^{19}F, 5n)^{174}Re. A self-supporting ^{160}Dy target of thickness 4.2 mg cm^{-2}, enriched to 79% purity and positioned at an angle of 70° to the beam, was irradiated by a pulsed beam of 107 MeV ^{19}F^{7+} ions that were produced by the 14 UD Pelletron and delivered to the target position with an average intensity of 1.4 e nA for approximately 100 hours. Beam pulses were $\approx$ 1 ns long, separated by 1.7 μs. Reaction products were stopped within the target where they deexcited and underwent radioactive decay.

The CAESAR array [6,7] surrounded the target position. During this experiment, CAESAR was composed of nine Compton-suppressed high-purity germanium (HPGe) detectors. All of these detectors were input into time-to-digital

 ©2020 American Physical Society

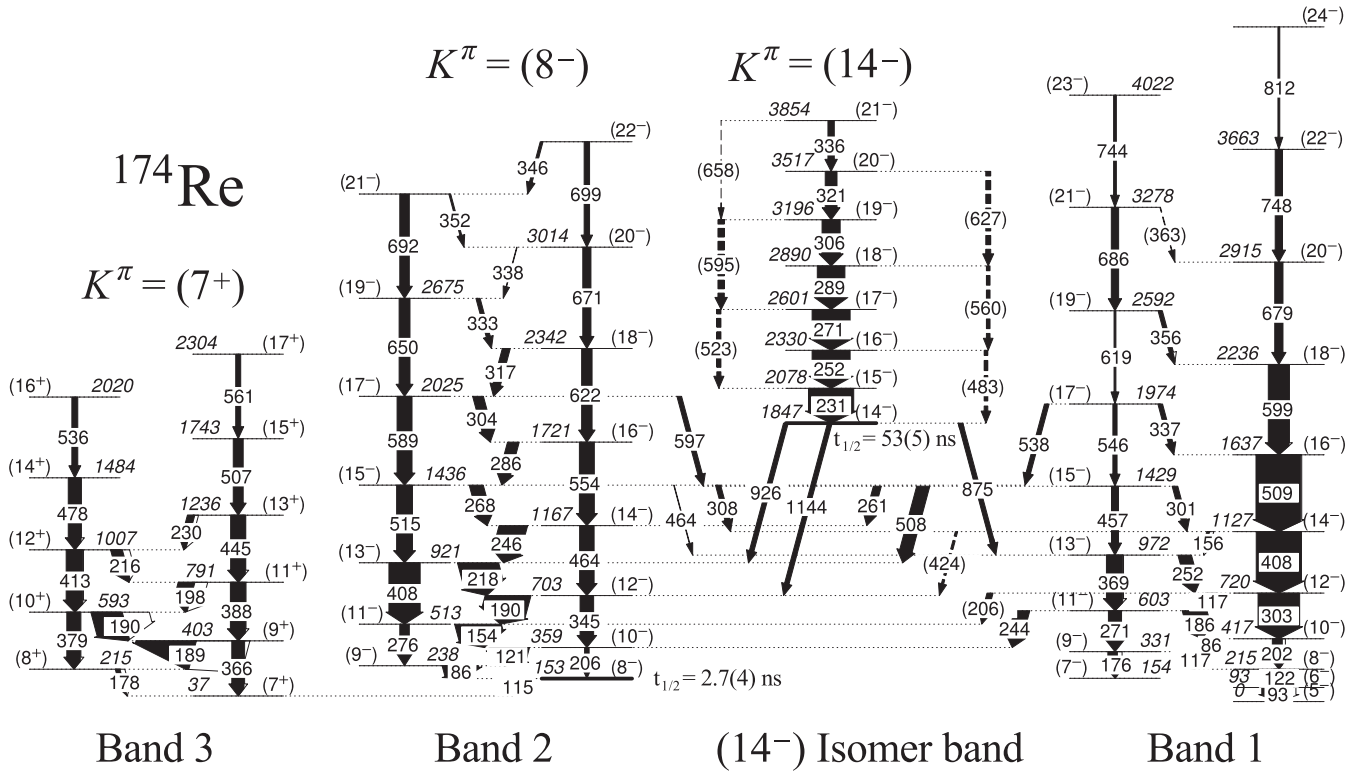

FIG. 1. Partial level scheme for ^{174}Re as based on γ-ray spectroscopy in this work, with state excitation energies relative to the bandhead of Band 1. The nomenclature used by Guo *et al.* [4] has been adopted here for ease of discussion. Bands 4 and 5 have been omitted from this figure. The intensities of transitions are indicated by the widths of the arrows. However, Bands 1 and 2 have been normalized separately to the isomer band and to Band 3.

converters (TDCs), which would output the time difference between signals from the corresponding detector and the beam pulse. This allows for γ-ray transitions to be investigated based on their temporal proximity to the initial reaction, a technique that is ideal for searching for states with lifetimes of order $\approx$100 ns.

As part of the analysis, demanding that γ-ray transitions occur between beam pulses restricts the observed transitions to those that have been delayed. These could be emitted following the decay of an isomeric state, in which case they may have originated from a reaction associated with the previous beam pulse, if the lifetime is not significantly longer than the pulse separation time. Alternatively, they could originate from the radioactive decay of activities accumulating at the target position, in which case they will not be correlated with the last beam pulse owing to the longer lifetimes of nuclear ground states in this region.

III. SPECTROSCOPY AND RESULTS

Prompt and delayed regions of the TDC spectra have been determined based on the presence of prompt γ-γ coincidences, which effectively vanish at a time >70 ns from the centroid of the prompt time peak. Accounting for the range of the TDCs, the total delayed region is 70–780 ns. Transitions present in this delayed time window must follow a long-lived state. Transitions at shorter times, in the 0–70 ns prompt time window, may originate from prompt cascades following directly from fusion-evaporation reactions, although delayed transitions may be seen here too. Correlations can be made between transitions occurring in the prompt time window, the delayed time window, and across both.

All of the previously reported bands associated with ^{174}Re [4], and the majority of the reported γ rays, have been observed in this experiment. The level scheme constructed in this work is shown in Fig. 1. For ease of discussion, the bands are labeled here using the nomenclature of Guo *et al.* [4].

A. New isomer band, $K^\pi = (14^-)$

In addition to its observation in the prompt time region, the lower-lying transitions in Band 2 have been observed in the delayed time region, Fig. 2(a), which is a signature of feeding from an isomeric state.

The prompt transitions feeding the isomer have been determined by selecting transitions that are seen only in the prompt time region, and are followed by transitions from Band 2 in the delayed time region. The resulting spectrum, Fig. 2(b), reveals that a band consisting of previously unobserved transitions is built on top of the isomer. Transitions of energy 231, 252, 271, 289, 306, 321, and 336 keV belong to this new isomer band, and are considered to be of $\Delta I = 1$ character. Corresponding $E2$, $\Delta I = 2$ transitions have not been unambiguously observed, and so are included tentatively in the level scheme with energies that have been calculated from the differences between excited states in the isomer band.

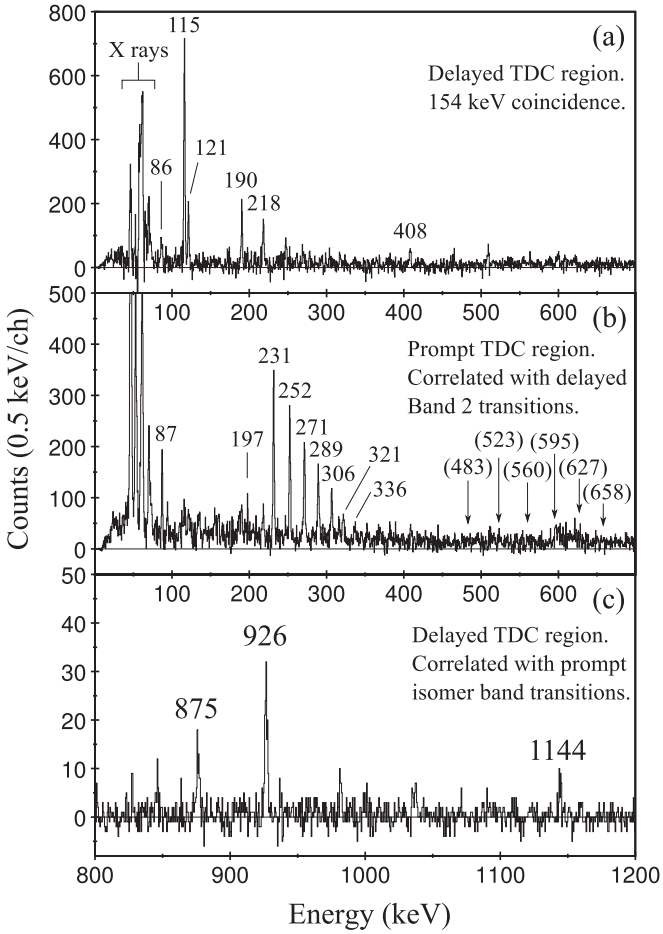

FIG. 2. (a) Energy spectrum of γ rays in the delayed TDC region, correlated with a 154 keV transition also in the delayed TDC region. Transitions at lower excitation energies in Band 2 can bee seen, indicating population from an isomeric state. (b) Energy spectrum of γ rays in the prompt TDC region, correlated with Band 2 transitions in the delayed TDC region. Transitions forming a band above an isomeric state can be seen. (c) Energy spectrum of γ rays in the delayed TDC region, correlated with the new isomer band transitions in the prompt TDC region. The labeled transitions depopulate the isomer. The origins of other features are described in the main text.

Nevertheless, their low intensities (see Table I), taken from their calculated locations, are valuable for constraining the g factors, which is discussed in Sec. IV.

Reversing this technique and looking for transitions in the delayed time region, preceded by transitions from the new isomer band in the prompt time region (231, 252, 271, 289 keV), confirms that Band 2 is indeed populated by the decay of this isomer. New delayed γ rays observed at higher energies, Fig. 2(c), correspond to transitions directly depopulating the isomer. These new transitions have been placed in the level scheme, shown in Fig. 1. Other features in Fig. 2(c) are contaminants that appear due to the large background relative to the gating transition intensity. The transition at 937 keV is in prompt coincidence with 185 and 281 keV transitions in ^{175}W, as well as characteristic tungsten x rays. The 981, 1034, and 1036 keV transitions are in prompt coincidence

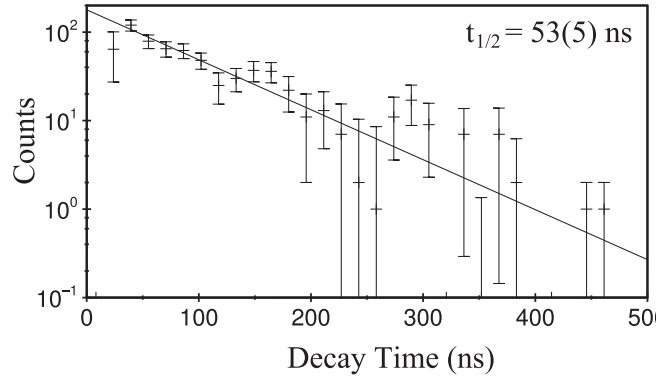

FIG. 3. Decay curve for the (14^-) isomer. The time differences between transitions in the band above the isomer and the 926 and 1144 keV transitions that depopulate the isomer are shown (0.781 × 20 ns per channel).

with the 113 and 243 keV transitions in ^{174}W, as well as tungsten x rays. However, the 937, 981, 1034, and 1036 keV transitions are not placed in the current level schemes for ^{174}W and ^{175}W [8,9].

A feature in Fig. 2(b) at a greater energy than the x rays is a γ-ray transition at 86.8 keV. It is in prompt coincidence with a 197 keV transition, labeled in Fig. 2(b), which is also in prompt coincidence with 297 and 385 keV transitions. This indicates that these transitions originated from ^{160}Dy, which was the target material.

A half-life for the isomer has been determined here for the first time by observing the time profile of the 926 and 1144 keV transitions, which directly depopulated the isomer. Observing these transitions gives a simple decay curve, shown in Fig. 3, as they exclusively depopulate the isomer, whereas transitions in Band 2 may be populated promptly, complicating the time profile. The half-life measured for the new isomer is 53(5) ns. A transition of energy 875 keV populates the 13^- state in Band 1 directly.

Adopting the spin and parity assignments for Band 2 made in [4], the spin and parity of the new isomer is assigned (14^-). Assuming 8^- for the bandhead of Band 2, the observation that the 1144 keV transition from the isomer bandhead is weak compared to the 926 keV transition [Fig. 2(c)] suggests a higher multipole order for the 1144 keV transition, i.e., $\lambda = 2$, compared to $\lambda = 1$ for the 926 keV transition. However, considering the 926/1144 keV pair, the $E1/M2$ combination is unlikely as it would be exceptional for an $M2$ transition to compete effectively with an $E1$ transition to the same rotational band when the half-life is in the ns range. Therefore, the $M1/E2$ combination is favored for the 926/1144 keV pair. This gives the spin-parity (14^-) assignment for the 53 ns isomer bandhead. The corresponding hindrance factors are discussed in Sec. IV.

B. The half-life of the bandhead of Band 2

Band 2 has been observed in this work, as well as in [4]. The bandhead of this structure is an (8^-) state, which is depopulated by a γ-ray transition of energy 115 keV. The

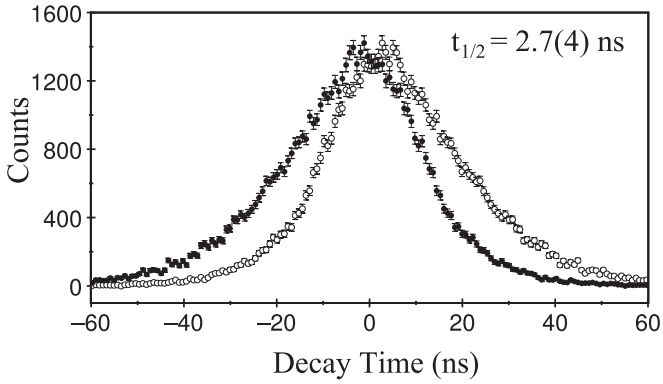

FIG. 4. Decay curves for the (8^-) bandhead of Band 2, corrected for time walk. Time differences between the transitions above the bandhead (154, 190, 218, 926, and 1144 keV) and the 115 keV transition that depopulates the 8^- state are shown (0.781 ns per channel). The mean lifetime from the centroid shift is 3.8(6) ns, giving a half-life of 2.7(4) ns.

half-life of the (8^-) state has been determined by observing the time differences between selected transitions above the bandhead (155, 190, 218, 926, and 1144 keV) and the 115 keV transition. The time differences are shown in Fig. 4, for both $t(\gamma_{115}) - t(\gamma_{\text{Band2}})$ and $t(\gamma_{\text{Band2}}) - t(\gamma_{115})$, indicating the mean lifetime of the state. Time walk affects the measurement of lower energy transitions such as the 115 keV transition. This has been accounted for by sampling the time behavior of the 121 keV transition, which is assumed to have a much shorter decay time while also having a similar energy to the 115 keV transition. The mean time walk is then subtracted from the time difference between 115 keV and the preceeding transitions. A half-life of 2.7(4) ns is measured for the (8^-) bandhead of Band 2. This measurement is significantly lower than that previously estimated [4].

The partial half-life of the γ-ray branch, which competes with internal conversion, has been determined using the theoretical internal conversion coefficient of 0.27 [11] for the 115 keV transition and, when compared to the Weisskopf estimate of 1.4×10^{-4} ns, gives a Weisskopf hindrance of $F_W^{E1} = 2.4(2) \times 10^4$. The equivalent state in ^{176}Re has a half-life of 30(3) ns and a Weisskopf hindrance of $F_W^{E1} = 2 \times 10^5$ [12], differing by one order of magnitude.

C. Branching ratios of transitions in Band 3

γ-ray transitions consistent with Band 3 in [4] have been observed in this experiment in the prompt time region. Previous work did not connect Band 3 to the rest of the level scheme, and suggested that it may have a four-quasiparticle configuration. No evidence has been observed to support this hypothesis in the present work. Indeed, it appears reasonable that the (7^+) state fed by Band 2 is in fact the bandhead of Band 3. This will be further discussed in Sec. IV A.

The relative intensities of γ-ray transitions depopulating each state have been determined by observing coincidences only with a transition directly populating that state, which has been possible for four states; see Table I. This has allowed g_K values to be determined, as discussed in Sec. IV.

IV. DISCUSSION

Much of what is revealed by γ-ray spectroscopy of ^{174}Re in this work is consistent with what has been previously published [4], and so a detailed discussion of all observable features is considered unnecessary. Instead, the focus will be on those areas where further insights have been enabled through new measurements, specifically from the spectroscopy of Band 3, the observation of a new isomer band, and the measurement of bandhead half-lives for Band 2 and the new isomer.

A. Band 3 configuration

The configuration of Band 3 was interpreted in previous work [4] as a four-quasiparticle configuration due to its large dynamic moment of inertia. Such a structure would

TABLE I. Measured γ-ray intensities and deduced g_K values of states in the new isomer band and in Band 3, with solutions for both positive and negative values of $(g_K - g_R)$. Energies of isomer band transitions labeled E_2 are calculated from the measured transitions labeled E_1, as are their uncertainties. Intensities of transitions at these energies were measured. Values of $g_R = 0.30(5)$ and $Q_0 = 6.5$ eb have been used [10].

I	E_1 (keV)	I_1	E_2 (keV)	I_2	g_K	g_K
Isomer band						
16	251.8(3)	84(6)	483.2(4)	8(5)	$0.61^{+0.26}_{-0.12}$	$-0.01^{+0.12}_{-0.26}$
17	270.6(3)	84(6)	523.2(4)	9(5)	$0.72^{+0.27}_{-0.14}$	$-0.12^{+0.13}_{-0.27}$
18	288.7(3)	61(6)	559.9(4)	8(6)	$0.80^{+0.57}_{-0.18}$	$-0.20^{+0.18}_{-0.57}$
19	305.9(3)	40(5)	595.8(4)	14(6)	$0.65^{+0.19}_{-0.12}$	$-0.05^{+0.12}_{-0.19}$
20	321.1(3)	26(5)	627.4(4)	11(5)	$0.67^{+0.22}_{-0.12}$	$-0.07^{+0.12}_{-0.22}$
Band 3						
9	188.7(3)	34(4)	366.2(3)	9(2)	$0.67^{+0.10}_{-0.09}$	$-0.07^{+0.09}_{-0.10}$
10	190.2(3)	21(2)	378.6(6)	16(2)	$0.60^{+0.07}_{-0.07}$	$-0.00^{+0.07}_{-0.07}$
11	198.2(3)	14(2)	388.4(3)	22(2)	$0.53^{+0.08}_{-0.07}$	$0.07^{+0.07}_{-0.08}$
12	215.6(3)	18(4)	413.4(3)	36(7)	$0.52^{+0.09}_{-0.08}$	$0.08^{+0.08}_{-0.09}$

TABLE II. Theoretical g_K values for the new isomer band, which has $K = 14$, and for Band 3, which has $K = 7$. An intrinsic spin quenching factor of 0.6 has been used. Values marked with * are shown in Fig. 6. The value marked with ** is shown in Fig. 5.

Configuration	Kg_K	g_K
Isomer band		
$\nu 7/2[633] \otimes \pi 5/2[402], \pi 9/2[514], \pi 7/2[404]$	12.813	0.915*
$\nu 5/2[512], \nu 7/2[514], \nu 7/2[633] \otimes \pi 9/2[514]$	4.867	0.348
$\nu 7/2[633], \nu 1/2[521], \nu 11/2[505] \otimes \pi 9/2[514]$	4.026	0.288*
Band 3		
$\nu 5/2[512] \otimes \pi 9/2[514]$	4.889	0.698**

have a bandhead at higher excitation energies than for two-quasiparticle configurations. In the absence of observable γ-ray transitions to lower energy states, an isomeric bandhead with a half-life greater than 1 μs was predicted based on the hypothesis that these transitions occurred outside of the experimental correlation time window of 200 ns [4]. In the present work, no evidence has been found to support the hypothesis that Band 3 is a four-quasiparticle band, and arguments supporting a two-quasiparticle configuration are presented in this section.

Band 3 is visible in prompt coincidence with the beam pulse. However, no transitions are observed in delayed coincidence with Band 3 across the delayed time window of 1.7 μs and so it is concluded that either Band 3 does not feed into the level scheme through a four-quasiparticle isomeric bandhead or that the half-life must be much longer than 1 μs in order to prevent the observation of delayed transitions. The longer half-life hypothesis can be ruled out by the lack of out-of-beam events, which would be observable in the delayed TDC region, belonging to the assigned two-quasiparticle bands of ^{174}Re.

The neighboring nucleus ^{176}Re [12] provides an interesting comparison with ^{174}Re due to the similar structures that can be seen in its level scheme. Analogous structures to those presented in this work are Bands A, B, C, and F, as designated in Ref. [12]. Band F has transition energies similar to those from Band 3 in ^{174}Re, in particular the 179.7 and 379.7 keV transitions to the bandhead, which are almost identical to the equivalent transitions in ^{174}Re. Band F has a bandhead spin and parity of (7^+), which is also expected in ^{174}Re (as will be described in Sec. IV C). The absence of observable transitions in delayed coincidence with Band 3 and the similarity to Band F in ^{176}Re suggest that Band 3 is a low-lying two-quasiparticle structure with a 7^+ bandhead. This is interpreted as the same state that is populated by the 115 keV transition from the (8^-) state in Band 2.

In the present work, a new isomer band has been observed. This reinforces the deduction that Band 3 is not analogous to the four-quasiparticle Band C in ^{176}Re, as the new isomer band is likely to be the analogous band in ^{174}Re.

Both the experimental and theoretical g_K values have been calculated using the methodologies described in [10]. In order to obtain g_K, the experimental values in Table I have been used to determine $(g_K - g_R)/Q_0$, which returns two solutions due to the presence of a quadratic equation in its derivation. These calculations have been made using values of $g_R = 0.3$ and $Q_0 = 6.5$ eb, which are consistent with the systematics of this region [10]. Conclusions based on these theoretical g_K values are insensitive, within uncertainties, to variations in Q_0 of up to 15%.

The theoretical estimates of g_K have been calculated based on possible Nilsson configurations. The relationship $Kg_K = \sum(\Lambda g_\Lambda + \Sigma g_\Sigma)$ is used, where Λ is the orbital angular momentum projection, Σ is the intrinsic spin projection, $g_\Lambda = 1$ or 0 for protons and neutrons respectively, and g_Σ is the free proton or neutron intrinsic spin value of 5.59 or -3.83 respectively, attenuated by a factor of 0.6. The Λ and Σ values are interpolated from the wave functions of Chi [13,14], using the calculated deformations (see Sec. IV C) assuming $\epsilon_2 = 0.95\beta_2$. The K quantum number for this band is 7. The resulting theoretical g_K values are shown in Table II and are plotted in Fig. 5. The g_K value for the $K^\pi = 7^+$ $\nu 5/2[512], \pi 9/2[514]$ configuration is consistent with the calculations (see also Sec. IV C). This configuration is adopted here for Band 3.

B. The $K^\pi = (14^-)$ isomer band configuration

A new band built upon an isomeric state has been observed in ^{174}Re for the first time in this work. The bandhead has an excitation energy of 1847 keV, relative to the bandhead of Band 1, as determined by the construction of the level scheme using early-delayed coincidences. As discussed in Sec. III, the spin and parity of the isomer is (14^-). The high spin of this bandhead requires a four-quasiparticle configuration.

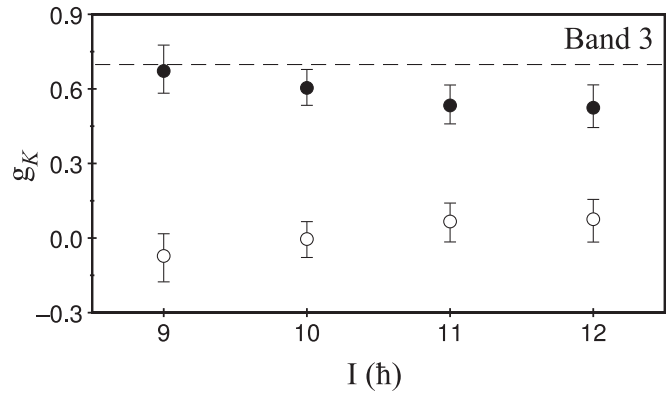

FIG. 5. Plot of g_K values for Band 3. Filled and clear circles correspond to g_K values calculated with the positive and negative $(g_K - g_R)/Q_0$ values respectively. The dashed line is the theoretical value for the $\nu 5/2[512], \pi 9/2[514]$ configuration.

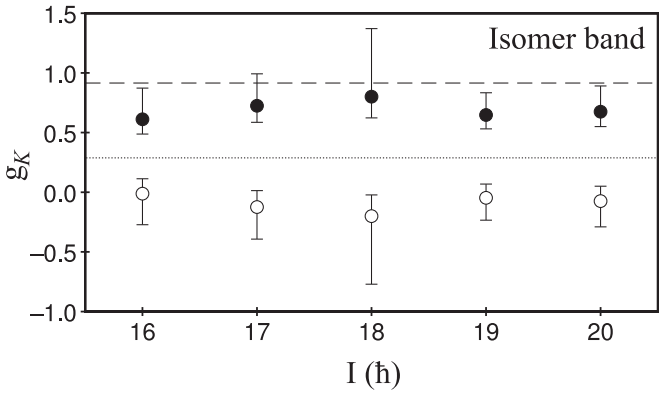

FIG. 6. Comparison of experimental g_K values for the isomer band with theoretical values. Filled and clear circles correspond to g_K values calculated with the positive and negative $(g_K - g_R)/Q_0$ values respectively. The theoretical values are for $1\nu 3\pi$ (dashed) and $3\nu 1\pi$ (fine dotted) configurations. The data align more closely with the $1\nu 3\pi$ g_K value.

In order to determine the underlying structure of this band, g_K values have been calculated from the experimental data shown in Table I, which have in turn been compared with theoretical g_K values for configurations in this region of the nuclear landscape (see Table II and Fig. 6). These values have been determined using the same methodology as for Band 3. The K quantum number for this band is 14.

The g_K of the $1\nu 3\pi$ configuration, $\nu 7/2[633]$, $\pi 5/2[402]$, $\pi 9/2[514]$, $\pi 7/2[404]$, is much more consistent with the experimental data than the $3\nu 1\pi$ configuration. Section IV C includes a comparison with calculated energies.

Although the $\Delta I = 2$ transitions in the isomer band are not firmly placed on the basis of well-defined peaks in the γ-ray spectra, their energies are known from the $\Delta I = 1$ transitions. In this circumstance, the intensities can be measured reliably, albeit with substantial uncertainties.

C. Potential energy surface calculations

Potential energy surface calculations have been performed using the configuration-constrained method of Xu *et al.* [16] to help identify the preferred configuration for the four-quasiparticle isomer (Fig. 7). A Woods-Saxon potential with universal parameters [17] and Lipkin-Nogami pairing were used. For each quasiparticle configuration, the occupied orbitals were fixed and the quadrupole and hexadecapole deformation parameters $(\beta_2, \gamma, \beta_4)$ were varied in order to minimise the excitation energies. The neutron and proton

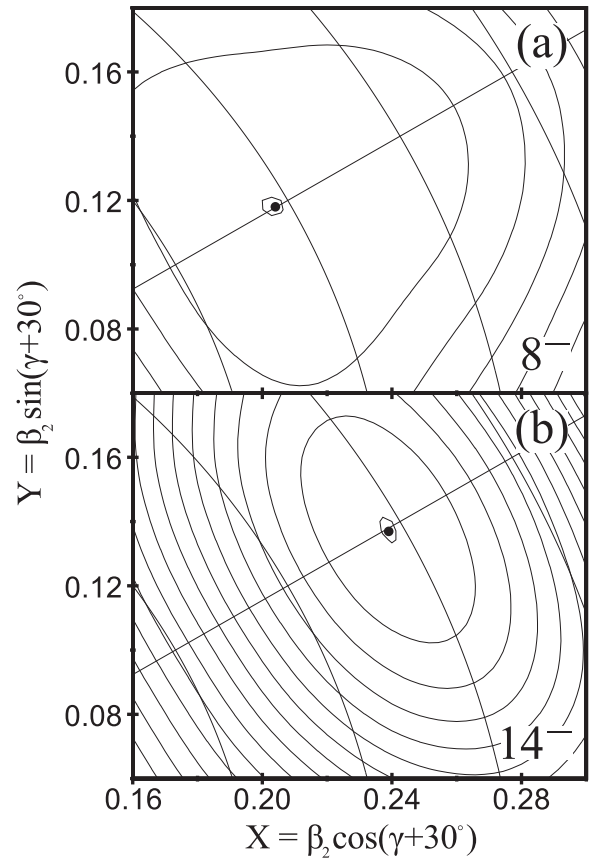

FIG. 7. Potential energy surface diagrams for nucleon configurations in ^{174}Re with K^π of (a) 8^- and (b) 14^-. The excitation energy is minimized at a greater β_2 deformation parameter for the 14^- configuration than for the 8^- configuration, as shown in Table III, possibly providing part of the mechanism for the isomerism of the 14^- state.

TABLE III. Theoretical excited states in ^{174}Re. For the two-quasiparticle states, the assigned K values are those favored by the Gallagher-Moszkowski rules [15].

K^π	Configuration	β_2	γ (deg.)	β_4	E'_{exc} (keV)
3^-	$\nu\frac{7}{2}^+[633] \otimes \pi\frac{1}{2}^-[541]$	0.251	0	0.005	28
4^+	$\nu\frac{1}{2}^-[521] \otimes \pi\frac{9}{2}^-[514]$	0.234	0	0.002	0
7^+	$\nu\frac{5}{2}^-[512] \otimes \pi\frac{9}{2}^-[514]$	0.217	0	−0.003	113
8^-	$\nu\frac{7}{2}^+[633] \otimes \pi\frac{9}{2}^-[514]$	0.235	0	0.002	85
14^-	$\nu\frac{7}{2}^+[633] \otimes \pi\frac{5}{2}^+[402], \pi\frac{9}{2}^-[514], \pi\frac{7}{2}^+[404]$	0.276	0	0.007	1785
14^-	$\nu\frac{5}{2}^-[512], \nu\frac{7}{2}^-[514], \nu\frac{7}{2}^+[633] \otimes \pi\frac{9}{2}^-[514]$	0.208	17	−0.011	2378
14^-	$\nu\frac{7}{2}^+[633], \nu\frac{1}{2}^-[521], \nu\frac{11}{2}^-[505] \otimes \pi\frac{9}{2}^-[514]$	0.269	0	0.004	1676
16^+	$\nu\frac{7}{2}^+[633] \otimes \pi\frac{5}{2}^+[402], \pi\frac{9}{2}^-[514], \pi\frac{11}{2}^-[505]$	0.212	0	−0.002	2651

TABLE IV. Hindrance factors for transitions depopulating the (14^-) isomer and the (8^-) bandhead in ^{174}Re. The branching ratios of transitions depopulating the (14^-) isomer have been determined from their intensity balance. For the transition depopulating the (8^-) state the branching ratio has been determined using theoretical internal conversion coefficients. Weisskopf hindrances and reduced hindrances are given. The stated multipole orders are those assumed for the hindrance factor calculations.

E_γ (keV)	Branching ratio	Multipolarity	$\frac{T_\gamma}{T_W}$	$(\frac{T_\gamma}{T_W})^{(1/\nu)}$	ν
From the (14^-) isomer					
875.1(3)	0.30(4)	$M1$	$5.1(8) \times 10^6$	4.7(1)	10
925.8(3)	0.54(5)	M1	$3.5(5) \times 10^6$	20.4(6)	5
(1127)	<0.02	$E2$	$>5 \times 10^5$	>4.3	9
1143.6(3)	0.16(3)	$E2$	$6.9(14) \times 10^4$	16.2(8)	4
From the (8^-) state					
115.4(3)	0.79	$E1$	$2.4(2) \times 10^4$	N/A	0

monopole pairing strengths were determined by the average gap method [18] with a 10% enhancement [16].

Of the calculated configurations, shown in Table III, three have a K^π of 14^- to match the isomer and have excitation energies of 1676, 1785, and 2378 keV. The two configurations with lower excitation energies are quite similar in energy, but the third configuration is over 500 keV higher in energy and as such has been ruled out as a likely configuration for the isomer.

Of the two lower-energy 14^- configurations, one is built upon $3\nu 1\pi$, while the other is $1\nu 3\pi$. In Sec. IV B, measurements of g_K were compared with theoretical values for configurations that would have $K^\pi = 14^-$ and it was concluded that the $1\nu 3\pi$ configuration was a more consistent fit with that data. In conjunction with the calculations presented in this section, the configuration of the isomer band is thus deduced to be $\nu 7/2[633], \pi 5/2[402], \pi 9/2[514], \pi 7/2[404]$.

A configuration of $K^\pi = 8^-$ has also been calculated. This configuration corresponds to Band 2, which is populated by the decay of the (14^-) isomer. The quadrupole deformation parameters (β_2) for these two configurations, shown in Table III, differ quite significantly, presenting a likely mechanism by which the isomerism of the 14^- configuration can be enhanced.

D. Reduced hindrance values

In this section, the reduced hindrance values are discussed for the isomeric γ-ray transitions listed in Table IV. These are determined [1,2] from the Weisskopf hindrance factors, $F_W = T^\gamma_{1/2}/T^W_{1/2}$, where $T^\gamma_{1/2}$ is the partial γ-ray half-life and $T^W_{1/2}$ is the corresponding Weisskopf single-particle estimate. The reduced hindrance is then evaluated as $f_\nu = (F_W)^{1/\nu}$, where $\nu = \Delta K - \lambda$ is the degree of forbiddenness of the transition. In this way, the reduced hindrance allows for the transition energy, multipole order and the degree of forbiddenness, so that variations in reduced hindrance are expected to reflect the different degrees of K mixing, with a large value of reduced hindrance ($f_\nu \approx 100$) indicating that K is conserved to a good approximation. It is notable that, where there are competing $M1$ and $E2$ transitions from a K isomer to a given rotational band, then the f_ν values tend to be similar, with $M1$ transitions typically having slightly larger f_ν values [1]. However, the $E2$ admixture in otherwise $M1$, $\Delta I = 1$ transitions is often unknown.

The central question to be addressed is the substantial difference in the γ-ray reduced hindrance factors from the $K^\pi = 14^-$ isomer to Band 2, with $K^\pi = 8^-$, compared to the transitions to Band 1, assigned $K^\pi = 3^-$ [4]. These are seen in Table IV to be $f_\nu = 20.4(6)$ ($M1$) and 16.2(8) ($E2$) to Band 2, compared to 4.7(1) ($M1$) and >4.3 ($E2$) to Band 1. Note that the 1127 keV, $E2$ transition to Band 1 remains unobserved, but we have obtained an upper limit for its intensity (<2%), and a corresponding lower limit for its reduced hindrance ($f_\nu >$ 4.3). Two scenarios are considered: first, the effect of mixing between Band 2 and Band 1; and second, the effect of the shape and configuration changes mediated by the transitions.

The mixing between Bands 1 and 2 is evident from the observed interband transitions, as has been discussed by Guo *et al.* [4]. For the present purposes, a spin-independent mixing matrix element, V, is assumed, and it is noted that the two $I^\pi = 15^-$ levels are $\Delta E = 7$ keV apart. In a two-band-mixing analysis, this determines that $V \leqslant 3.5$ keV. Considering the maximum value (consistent with Ref. [4]) and applying it to the mixing at $I^\pi = 13^-$, where the two states are $\Delta E =$ 51 keV apart, the fraction of the Band 2 wave function mixed into Band 1 can be obtained (for small values) as $\beta^2 \approx V^2/(\Delta E)^2 = 0.005$. Allowing for the different γ-ray transition energies from the $K^\pi = 14^-$ isomer, the expected contribution of the less-forbidden Band 2 ($M1$, $\nu = 5$) component to the transition to Band 1 would be only 1% of its measured intensity. Therefore, this kind of band mixing does not play a significant role in explaining the different reduced hindrance factors.

Another possibility is that the deformation and configuration differences are important. The β_2 deformation of the $K^\pi = 14^-$ isomer is calculated (Table III) to be 0.276, compared to the populated $K^\pi = 8^-$ and 3^- bands with $\beta_2 =$ 0.235 and 0.251 respectively.

The effects of β_2 deformation changes on high-K isomer decay rates have hardly been discussed in the literature. In their calculations of the shapes of $K^\pi = 8^-$ isomers in $N = 74$ and $N = 106$ isotones, Xu *et al.* [19] point out that, as the $Z = 50$ and 82 closed shells are approached, the increasing hindrance factors could reflect the shape differences between the isomers and their respective ground states. However, in

the well deformed regions away from closed shells, shape-difference effects on f_ν have not been previously identified.

Considering the $A \approx 180$ and 250 well-deformed regions of high-K isomers, the shapes of multi-quasiparticle, high-K states have been calculated for a limited number of nuclides, in particular (in order of publication date) ^{178}W and ^{182}Os [16,20], ^{183}Re [21], ^{190}W [22], ^{184}Os [23], ^{181}Os [24], ^{180}Re [3], ^{254}No [25], favored states in the ^{250}No–^{272}Cn region [26], and ^{174}Re (this work). It is notable that, of all the possible β_2 shape changes between the high-K configurations, the largest is for ^{174}Re, and, indeed, the largest multiquasiparticle β_2 value (0.276) is for the presently discussed $K^\pi = 14^-$ isomer.

The reason for the large $K^\pi = 14^-$ isomer deformation can be seen from the available Nilsson orbitals close to the proton Fermi surface, as illustrated in, for example, the Nilsson diagrams in Ref. [16]. With $Z = 75$ and single occupancy of all three of the 5/2[402], 7/2[404], and 9/2[514] orbitals (see the configuration in Table III) there has to be double occupancy of the strongly deformation-driving 1/2[541] proton orbital, and such double occupancy is not associated with the other ^{174}Re configurations. It is also interesting to see in Table III that single occupancy of that orbital in the Band-1 ($K^\pi = 3^-$) configuration leads to its large deformation ($\beta_2 = 0.251$) but not as large as for the double occupancy in the isomer configuration ($\beta_2 = 0.276$).

In ^{174}Re, we can therefore correlate the relatively low reduced hindrance to Band 1, which is significantly lower than for the transitions to Band 2, with the deformation change, which is relatively small for transitions to Band 1 compared to Band 2. In ordinary circumstances, the transitions to Band 1 would be much less intense, on account of the greater degree of K forbiddenness (compared to the transitions to Band 2), but competition is evidently possible in the present case. At first sight, this may be related to the large deformation change required for transitions to Band 2, causing extra inhibition for that decay pathway. However, any deformation changes are associated with configuration changes, and in this case the emptying of the doubly occupied 1/2[541] proton orbital in the decay process may in itself be the key factor.

It is hoped that further information of this kind will, in the future, help to clarify the important degrees of freedom, but it is notable that, of all the rhenium four-quasiparticle isomers so far studied [1], the $K^\pi = 14^-$ isomer of ^{174}Re is unique in involving three protons, so that it may have a uniquely large β_2 deformation change in its K-forbidden decay. (While there are many three-proton cases in the tantalum isotopes, the $Z = 73$ Fermi surface does not then require the double occupancy of the 1/2[541] proton orbital). It would clearly be valuable to make a more quantitative calculation to see if the relatively large transition hindrance can indeed be explained as being due to the proposed β_2 deformation change and the associated orbital rearrangements.

V. SUMMARY

With pulsed-beam facilities, new isomer data have been obtained for ^{174}Re, including a rotational band based on a four-quasiparticle state with a half-life of 53(5) ns. The isomeric decay of the bandhead populates two different two-quasiparticle bands. The decay reduced hindrance factors differ significantly, as do the calculated β_2-deformation changes. The change in the degree of occupation of the 1/2[541] proton orbital is suggested to be the key physical influence.

ACKNOWLEDGMENTS

The technical staff at the ANU 14UD accelerator facility are thanked for their excellent support. Funding is acknowledged from the UK Science and Technology Facilities Council under Grant No. ST/P005314/1. A.A. and M.S.M.G. acknowledge the support of the Australian Government Research Training Program. This research was supported by the Australian Research Council through Grants No. DP120101417 and No. DP130104176. Support for the ANU Heavy Ion Accelerator Facility operations through the Australian National Collaborative Research Infrastructure Strategy (NCRIS) program is acknowledged.

[1] F. G. Kondev, G. D. Dracoulis, and T. Kibédi, At. Data and Nucl. Data Tables **103-104**, 50 (2015).
[2] G. D. Dracoulis, P. M. Walker, and F. G. Kondev, Rep. Prog. Phys. **79**, 076301 (2016).
[3] H. M. El-Masri, P. M. Walker, G. D. Dracoulis, T. Kibédi, A. P. Byrne, A. M. Bruce, J. N. Orce, A. Emmanouilidis, D. M. Cullen, C. Wheldon, and F. R. Xu, Phys. Rev. C **72**, 054306 (2005).
[4] S. Guo, Y. H. Zhang, X. H. Zhou, M. L. Liu, Y. X. Guo, Y. H. Qiang, Y. D. Fang, X. G. Lei, F. Ma, M. Oshima *et al.*, Phys. Rev. C **86**, 014323 (2012).
[5] G. D. Dracoulis, Nucl. Phys. News **9**, 9 (1999).
[6] G. D. Dracoulis and A. P. Byrne, Australian National University Technical Report No. ANU-P/1052, 1995 (unpublished), p. 115.
[7] T. P. D. Swan, P. M. Walker, Z. Podolyak, M. W. Reed, G. D. Dracoulis, G. J. Lane, T. Kibédi, and M. L. Smith, Phys. Rev. C **83**, 034322 (2011).
[8] S. K. Tandel, P. Chowdhury, E. H. Seabury, I. Ahmad, M. P. Carpenter, S. M. Fischer, R. V. F. Janssens, T. L. Khoo, T. Lauritsen, C. J. Lister *et al.*, Phys. Rev. C **73**, 044306 (2006).
[9] P. M. Walker, G. D. Dracoulis, A. Johnston, J. R. Leigh, M. G. Slocombe, and I. F. Wright, J. Phys. G **4**, 1655 (1978).
[10] P. M. Walker, G. D. Dracoulis, A. P. Byrne, B. Fabricius, T. Kibédi, and A. E. Stuchbery, Nucl. Phys. A **568**, 397 (1994).
[11] T. Kibédi, T. W. Burrows, M. B. Trzhaskovskaya, P. M. Davidson, and C. W. Nestor, Jr., Nucl. Instrum. Methods A **589**, 202 (2008).

[12] M. A. Cardona, A. J. Kreiner, D. Hojman, G. Levinton, M. E. Debray, M. Davidson, J. Davidson, R. Pirchio, H. Somacal, D. R. Napoli *et al.*, Phys. Rev. C **59**, 1298 (1999).
[13] B. E. Chi, Nucl. Phys. **83**, 97 (1966).
[14] B. E. Chi, Nucl. Phys. **89**, 706 (1966).
[15] C. J. Gallagher and S. A. Moszkowski, Phys. Rev. **111**, 1282 (1958).
[16] F. R. Xu, P. M. Walker, J. A. Sheikh, and R. Wyss, Phys. Lett. B **435**, 257 (1998).
[17] J. Dudek, Z. Szymański, and T. Werner, Phys. Rev. C **23**, 920 (1981).
[18] P. Möller and J. R. Nix, Nucl. Phys. A **536**, 20 (1992).
[19] F. R. Xu, P. M. Walker, and R. Wyss, Phys. Rev. C **59**, 731 (1999).
[20] D. M. Cullen, S. L. King, A. T. Reed, J. A. Sampson, P. M. Walker, C. Wheldon, F. Xu, G. D. Dracoulis, I.-Y. Lee, A. O. Machiavelli, R. W. MacLeod, A. N. Wilson, and C. Barton, Phys. Rev. C **60**, 064301 (1999).
[21] C. S. Purry, P. M. Walker, G. D. Dracoulis, S. Bayer, A. P. Byrne, T. Kibédi, F. G. Kondev, C. J. Pearson, J. A. Sheikh, and F. R. Xu, Nucl. Phys. A **672**, 54 (2000).
[22] Z. Podolyák, P. H. Regan, M. Pfützner, J. Gerl, M. Hellström, M. Caamaño, P. Mayet, C. Schlegel, A. Aprahamian, J. Benlliure *et al.*, Phys. Lett. B **491**, 225 (2000).
[23] C. Wheldon, G. D. Dracoulis, R. T. Newman, P. M. Walker, C. J. Pearson, A. P. Byrne, A. M. Baxter, S. Bayer, T. Kibédi, T. R. McGoram *et al.*, Nucl. Phys. A **699**, 415 (2002).
[24] D. M. Cullen, L. K. Pattison, J. F. Smith, A. M. Fletcher, P. M. Walker, H. M. El-Masri, Z. PodolyÃ¡k, R. J. Wood, C. Scholey, C. Wheldon *et al.*, Nucl. Phys. A **728**, 287 (2003).
[25] H. L. Liu, F. R. Xu, P. M. Walker, and C. A. Bertulani, Phys. Rev. C **83**, 011303(R) (2011).
[26] H. L. Liu, P. M. Walker, and F. R. Xu, Phys. Rev. C **89**, 044304 (2014).